Microsyst Technol (2007) 13: 487–493
DOI 10.1007/s00542-006-0201-4

TECHNICAL PAPER

K. D. Vora · A. G. Peele · B.-Y. Shew
E. C. Harvey · J. P. Hayes

Fabrication of support structures to prevent SU-8 stiction in high aspect ratio structures

Received: 31 August 2005 / Accepted: 20 January 2006 / Published online: 30 May 2006
© Springer-Verlag 2006

Abstract We have previously demonstrated that it is possible to fabricate densely-packed high aspect ratio structures in SU-8 by means of a top-plate support member which stiffens the overall structure and prevents pattern collapse. In this work we have computed the tensile stresses induced in the top-plate structures due to the capillary forces that arise between the columns due to the surface tension of the drying liquid. We have further studied the dynamic behavior of the structure after an instantaneous force. Based on these results, we have shown that the predicted optimal thickness of the top-plate structure is sufficient to maintain structural integrity.

Keywords Deep X-ray lithography · Densely packed high aspect ratio structures · Stiction

1 Introduction

Deep X-ray Lithography (DXL) is a technique used to produce high aspect ratio submicron, micron or mm structures with high resolution (Ehrfeld and Lehr 1995; Guckel 1996; Kupka et al. 2000). High energy (> 1 keV) synchrotron radiation (X-rays) with wavelengths as low as 0.5 nm are used to define patterns in the X-ray photoresist using an X-ray mask. The resist is then developed and depending on the tone of the resist, positive or negative features are produced. The developed areas are electroplated often using nickel or copper and the resist is removed to yield the metal part, which can be either final product or can be used as a mold for injection molding or hot embossing as in the original LIGA process (Kupka et al. 2000).

SU-8 is a negative-tone epoxy-type, UV photoresist that can be patterned to produce high aspect ratio structures with near vertical sidewalls. Various exposure techniques, including UV, X-ray, e-beam and proton beam, have been demonstrated (LaBianca and Gelorme 1997; Bogdanov and Peredkov 2000; Cheong et al. 2004; Chammika et al. 2003). UV lithography is by far the most common exposure technique or patterning SU-8 (LaBianca and Gelorme 1997; Shaw et al. 1997; Despont et al. 1997). However, due to optical diffraction, it is not possible to fabricate high aspect ratio structures with the same quality when the resist thickness exceeds 500 µm. Use of SU-8 photoresist for very high aspect ratio X-ray lithography was first investigated by Bogdanov in 1998 (Bogdanov and Peredkov 2000). Since then, it has been proved that the resolution and quality of SU-8 using X-ray lithography is as good as PMMA (Jian et al. 2003) and its sensitivity is 70 times greater (Singleton et al. 2001).

In MEMS fabrication, the adhesion of microstructures to the substrate during the drying step after wet etching of the sacrificial layer is termed as ‘stiction’ (Alley et al. 1992). The cause of stiction is attributed to the surface tension force of the rinse liquid trapped in the small space between the substrate and microstructure (Nathanson and Guldberg 1975). The magnitude of these forces is strongly dependent on the surface tension of the rinse liquid and the gap between the substrate and microstructure. Depending on the stiffness of the microstructure, they will be released from the substrate or adhere to the substrate permanently (Mastrangelo 1997). Several authors have proposed theoretical models to explain this phenomenon (Alley et al. 1992; Nathanson and Guldberg 1975; Mastrangelo 1997;

K. D. Vora (✉) · A. G. Peele
Department of Physics, La Trobe University,
Bundoora 3086, Australia
E-mail: kdvora@students.latrobe.edu.au
Tel.: +61-3-94792651
Fax: +61-3-94791552

B.-Y. Shew
Device Technology Group, National Synchrotron
Radiation Research Center, 101, Hsin-Ann Rd,
30077 Hsinchu SBI Park, Taiwan

E. C. Harvey · J. P. Hayes
Industrial Research Institute of Swinburne,
Swinburne University of Technology, 543-545 Burwood Road,
Hawthorn, VIC 3122, Australia

Raccurt et al. 2004; Niels et al. 1996; Maboudian and Howe 1997).

In our case, we wish to fabricate high aspect ratio structures (HARS) consisting of long, densely-packed channels for their potential application as X-ray reflective optics (Kupka et al. 2003; Peele et al. 2002). Other applications include mammography (Makarova et al. 2003; Fischer et al. 2000) and gamma-ray (Makarova et al. 2004) collimator grids and channels for electrophoresis (Fujimura et al. 2003). While it is possible to fabricate high aspect ratio isolated structures (Friedrich et al. 1997) it is a more difficult task to create structures where there is a densely-packed array of free-standing high aspect ratio structures. The surface tension from the rinse liquid present in the small gaps between the columns creates capillary forces that make the columns likely to suffer from the same type of stiction problem as seen in traditional MEMS fabrication. Other authors have also considered densely-packed high aspect ratio structures in SU-8 and have characterized various process parameters (Becnel et al. 2005). In previous work (Peele et al. 2004), some of us demonstrated that a support structure at the top of the channels can be used to prevent the movement of structures and hence, stiction in densely-packed HARS. We have further analyzed the mechanical properties of the support structures and have demonstrated optimal (or minimal) thickness structures that can prevent pattern collapse in our densely-packed HARS.

In this work, we first outline our theoretical result of when stiction becomes an issue in HARS (Vora et al. 2005). We present new studies demonstrating the expected tensile stresses in the support structures and how this relates to the failure of those structures and consequent stiction. We also consider a simple dynamical scenario showing vibrations in the array as a result of impulse loading from a rapid change in surface tension forces.

2 Review

Figure 1 shows four square columns with length, L, and width, w, separated from each other by a gap, g. As we have previously discussed (Vora et al. 2005), each column can be considered as a cantilever, which is subjected to a pressure due to capillary forces arising from the fluid between the two columns. In a real array fluid levels on different sides of a column may become uneven due to factors such as contaminants and asymmetry in the structures. There will also be a force imbalance at the edge of the array where columns have no outside neighbor. Accordingly, we treat the case of the 2×2 array of columns with a capillary fluid on the inside surfaces only as producing an upper limit on the forces involved.

By means of considering the maximum deflection, $\delta_{\max}$, arising from the pressure imbalance between the interstitial rinse fluid and the air we have shown that:

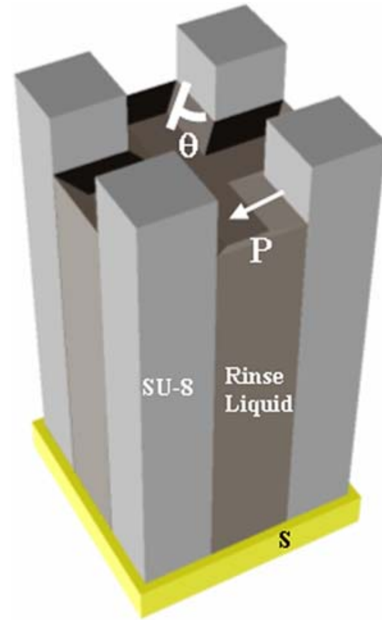

Fig. 1 Four columns of length L and width, w attached to a substrate, S, separated by a gap, g, experience a capillary pressure which tends to stick them together. The fluid forms a meniscus with a contact angle of θ to the column

$$\delta_{\max} = \frac{6\gamma \cos\theta L^4}{Egw^3} \quad (1)$$

where γ is the surface tension of the final rinse liquid and E is the Young's modulus of the column material ($E_{\mathrm{SU-8}} = 2.7$ Gpa ; Matthew et al. 2003). We used isopropyl-alcholol (IPA) with $\gamma = 21.7 \times 10^{-3}\ \mathrm{Nm}^{-1}$ and $\theta = 90°$ as the final rinse liquid (Raccurt et al. 2004).

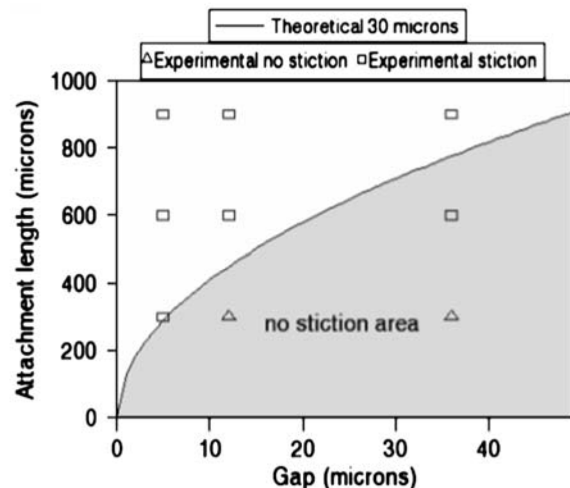

Fig. 2 Graph of attachment length as function of gap between columns for **a** 50 µm, **b** 30 µm and **c** 10 µm *square columns*. The experimental results are shown by *squares* where the structure collapsed and by *triangles* where the structures were freely standing. The *two squares below* the curve in (**a**) and (**b**) indicate that the structures collapsed despite being shorter than the theoretical attachment length

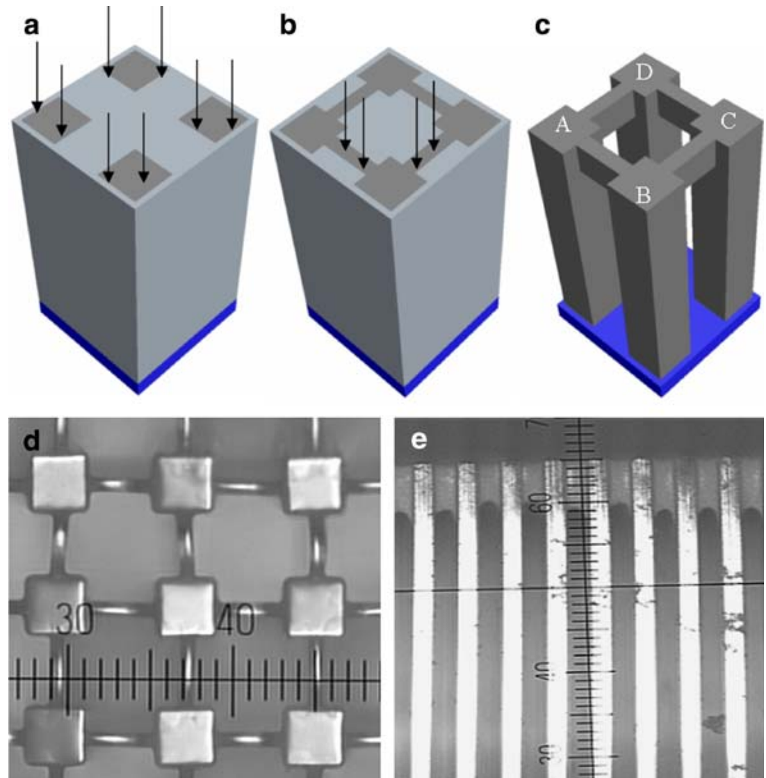

Fig. 3 Top-plate process steps. **a** X-ray exposure through an X-ray mask. **b** Low-dose UV exposure using a mask that links the structures exposed in step **a** and **c** develop. Microscope *top view* **d** and *side view* **e** of 50 μm *square columns*, 1.5 mm tall with a 60 μm gap and 70 μm thick top-plate

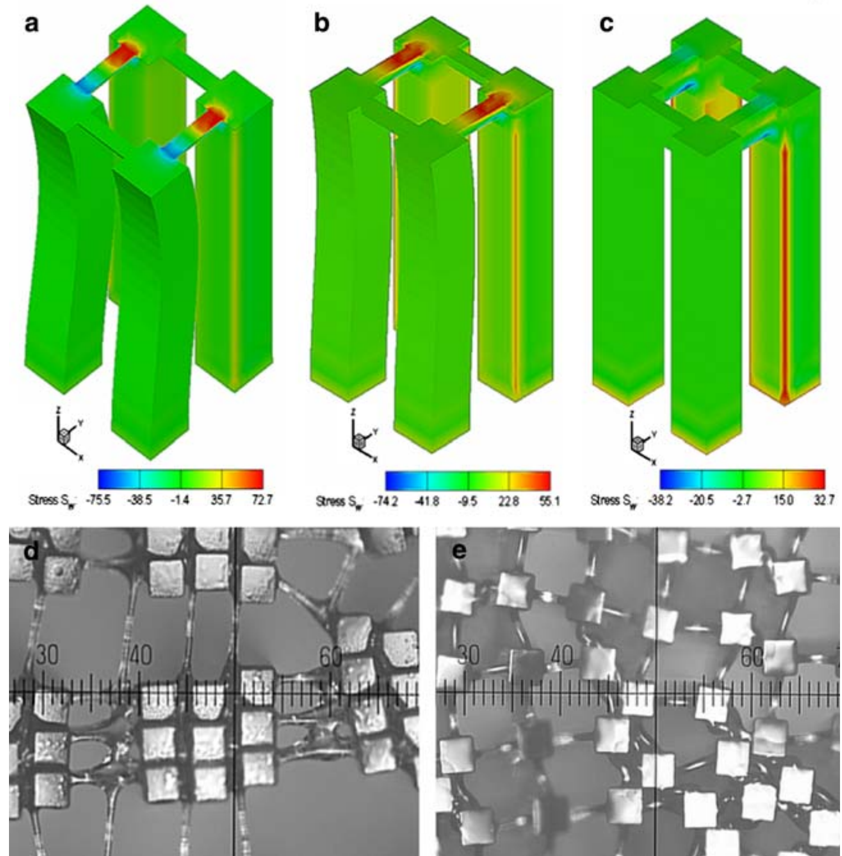

Fig. 4 Simulation results to determine tensile stress in top-plate structure with thickness of **a** 15 μm, **b** 30 μm and **c** 70 μm. The columns are 50 μm wide, 1.5 mm tall with gap of 60 μm between them. The *z*-scale is demagnified by factor of 0.5 whereas the *x* and *y* scale are magnified by factor of 3. Microscope *top view* of the structures with top-plate thickness of **d** 35 μm and **e** 50 μm

Fig. 5 Time-series results for 900 μm high, 30 μm square arrays with a 12 μm gap and a 135 μm thick properly aligned top-plate **a** after 1.3 ms, **b** after 2.9 ms, **c** after 6 ms and **d** after an infinite time of an impulse force

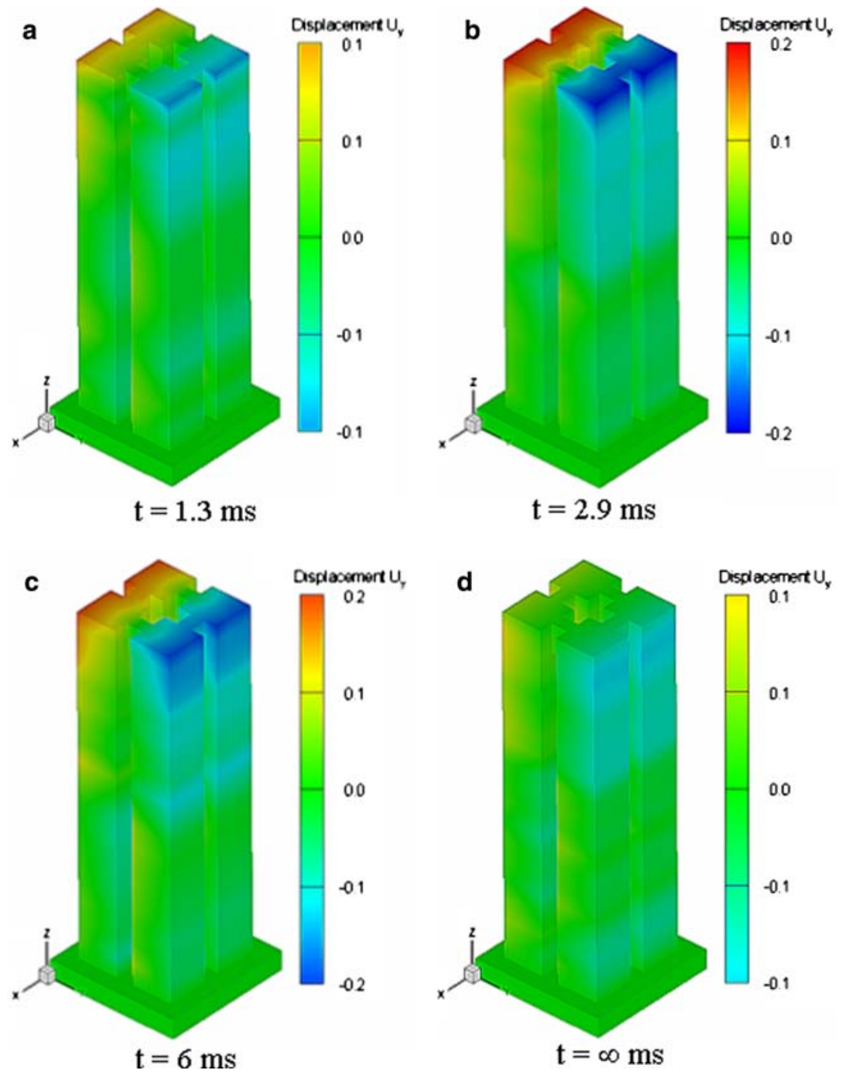

Now, L/w is the aspect ratio of the features in the structure, A_f and L/g is the aspect ratio of gap between columns, A_g. Putting this into Eq. 1 we get:

$$\delta_{\max} = \frac{6\gamma \cos\theta A_\mathrm{f}^3 A_\mathrm{g}}{E}. \qquad (2)$$

It can be seen that as the spacing between the features increases, the deflection decreases. In the absence of effects such as tip shear and column surface adhesion, the structures are likely to attach to each other if the deflection is equal to or more then the gap. We define an attachment length, L_a, as being the height of the column above which the deflection is greater than half the gap between the columns. Substituting $\delta_{\max} = g/2$ in Eq. 2 and solving for length we have:

$$L_\mathrm{a} = \left(\frac{Eg^2w^3}{12\gamma\cos\theta}\right)^{\frac{1}{4}}. \qquad (3)$$

We have demonstrated that this approach gives a reliable lower limit to the estimated attachment length. Figure 2 shows a graph of our attachment length as a function of gap for 30 μm square channels. The solid symbols are the calculated points for the column widths and gaps considered in our experimental work. It can be seen from Fig. 2 that as the gap increases so too must the aspect ratio of the structure in order that the columns do not attach. Using this curve we predict that structures that fall in the unshaded area will suffer from pattern collapse due to stiction. It is precisely these structures that will benefit from the mechanical stiffening provided by our top-plate support structures.

3 Support structures

In our previous work (Peele et al. 2004), we have fabricated support structures, which we refer to as a 'top-plate' to prevent stiction in densely-packed HARS using a second low-dose UV exposure into the same X-ray exposed resist. The design of the top-plate mask is a reverse of the square hole pattern so that a grid of lines is

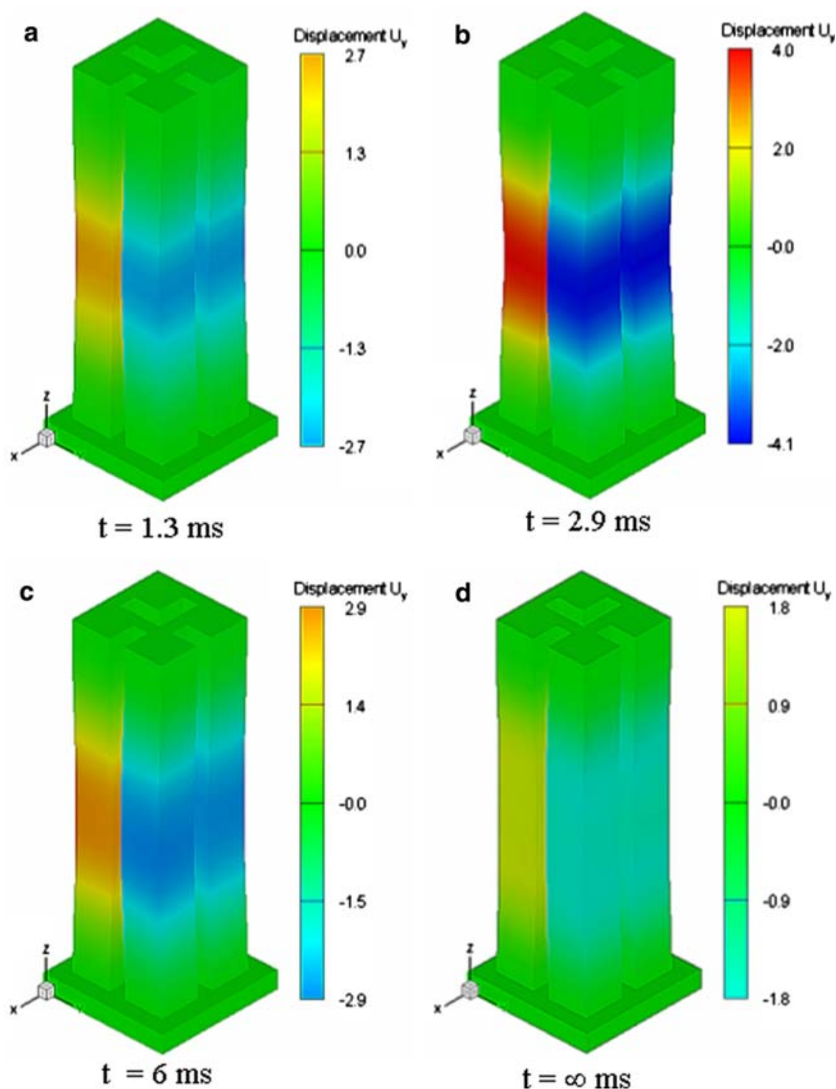

Fig. 6 Time-series results for 900 μm high, 30 μm square arrays with a 12 μm gap and a 135 μm thick top-plate misaligned at the edges **a** after 1.3 ms, **b** after 2.9 ms, **c** after 6 ms and **d** after an infinite time of an impulse force

exposed in the resist. The UV dose is kept low enough so that the cross-linking occurs to a shallow depth. This results in a bridge-like structure between the adjacent columns, which helps prevent them from collapsing. Figure 3 a–c shows the steps in fabrication of densely-packed columns with a top-plate support. Figure 3d, e show an experimental example of the resulting top-plate structure.

3.1 Tensile Stress

Once it is known that a top-plate is required, it is important to determine its minimal thickness. Thinner top-plates will break during the drying step while excessive top-plate thickness is wasteful as in some structures the top-plate is removed at the final process step. The structure shown in Fig. 3c is similar to 3D frame structures

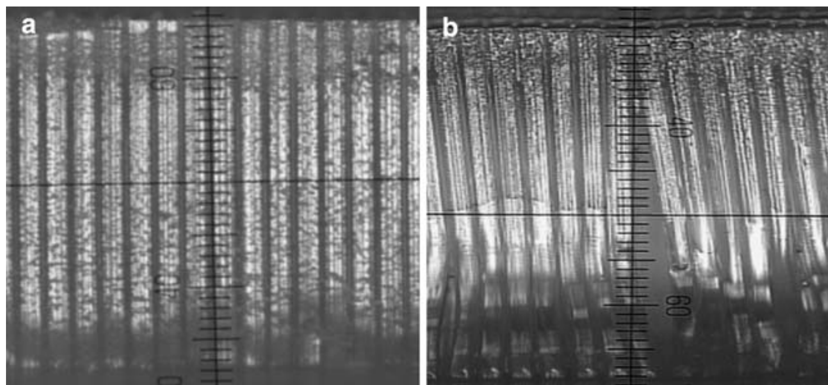

Fig. 7 Microscope images of the structures **a** corresponding to Fig. 5 and **b** corresponding to Fig. 6

used in civil engineering. In an ideal array of such columns, the net capillary force would be zero. However, as mentioned above, in a real array, fluid levels on different sides of columns may become uneven due to factors such as contaminants and asymmetry in the structures. Let us take an extreme case whereby columns A and B (Fig. 3d) experience a net force in the direction of column C and D as well as between them. We also assume that the net force on columns C and D is equal in all directions. Columns A and B will therefore be pulled towards columns C and D. Because the columns are fixed at the bottom and supported at the top, the middle portion of the columns A and B will suffer the greatest stress. This in turn produces a reaction force at the top and bottom of the columns, which thereby produces tensile stress in the top-plate structures. The magnitude of the tensile stress will depend on the area of the cross-section of the top-plate structure. The lateral width of the top-plate was chosen to be one-third of the feature size so that the developer can penetrate into the array with minimal obstruction from the support structure. Since, the width is fixed, the cross-sectional area of the top-plate can be changed only by changing its thickness. The ultimate tensile strength of SU-8 resin is $\sim$ 50 MPa (Ru Feng and Farris 2003). If the tensile stress in the top-plate is more then 50 MPa, the top-plate will break or plastically deform and the columns are likely to stick together. We have used a finite elements approach to determine the stress induced in the support structures and hence, to predict the minimum top-plate thickness required for a given feature size and spacing for an aspect ratio of 30. Figure 4a–c shows the tensile stress developed in the top-plate structures with thickness of 15, 30 and 70 μm for 1.5 mm long 50 μm square column.

It can be seen from Fig. 4 that as the thickness of the top-plate structure increases, the magnitude of tensile stress decreases. For top-plates with a thickness of 15 and 30 μm, the tensile stress is higher than the tensile yield of SU-8 and we predict that the top plate will either deform permanently or eventually break. This is demonstrated experimentally as can be seen in Fig. 4d, e. Another interesting observation from the experimental result is that for thin top-plate supports the structures will attach as seen in Fig. 4d whereas if the thickness is increased (but is still below the minimal required thickness for structural integrity) then the structure will deform but the top-plate still acts to prevent adhesion (see Fig. 4e). This is suggestive that in Fig. 4d the ultimate tensile yield is exceeded whereas in Fig. 4e we are in the plastic deformation region, which is in reasonable agreement with the simulations. For the top-plate with a thickness of 70 μm, the tensile stresses are well below the tensile yield of SU-8. This thickness would therefore be sufficient to prevent pattern collapse as seen in Fig. 3d, e.

3.2 Dynamics

The capillary force arising due to the surface tension of the drying liquid is transient; that is it is not permanent. We modeled an extreme case whereby the capillary force on one side of channels A and B (Fig. 3c) is instantaneously removed. This impulse force will cause the microstructure to vibrate. Our simulations show that the middle portion of the column is displaced more during the vibration. The top-plate thickness should be designed so that it does not break or deform under the impulse load and so that it is sufficient enough to restrict the maximum displacement during the vibration to less then half the gap. After determining the required top-plate thickness we used our finite element approach to calculate the system stresses and strains as a function of time after the application of the impulse force. We found that the minimal top-plate thickness that was estimated in the static case is sufficient to withstand the maximal impulse. In this case lateral vibrations are observed as well as vertical motion due to the column bending. Figure 5 shows a time-series for an array of 30 μm wide and 1 mm tall columns with 12 μm spacing and a top-plate thickness of 135 μm. It can be seen that the structure survives the impulse. If the top-plate thickness is reduced sufficiently then large lateral and vertical vibrations sufficient to cause deformation in the columns is observed.

During the UV exposure of the top-plate structures, which takes place after the X-ray exposure, there is a possibility of misalignment such that the top-plate is not exactly in the middle of the structures. This case was also modeled to find out the effect of misalignment. Figure 6a–d shows the simulation results of a time-series analysis for an array with the same dimensions as in Fig. 5 but without proper top-plate alignment. Figure 7a, b show experimental examples corresponding to the simulations in Figs. 5 and 6, respectively. Figure 6a–d shows the displacement after 1.3, 2.9, 6 ms and an infinite time after the impulse force, respectively. The maximum displacement was found at 2.9 ms and is equal to 4.1 μm, much less then half the gap. Upon relaxation, however the column is permanently bent as seen in Figs. 6d and 7b. For the aligned case, the displacement was found to be constant and almost negligible in the lateral direction and this was verified experimentally (Fig. 7a). It is seen clearly from Fig. 6 that the maximum displacement occurs at the mid-height of the columns when the top-plate is misaligned. When the top-plate is aligned properly, the displacement is an order of magnitude smaller than for the misaligned case (Fig. 5). Hence, to prevent pattern collapse, the top-plate thickness for the misaligned case would need to be thicker then that for the aligned case.

4 Conclusions

We have extended our process work that predicted the onset of stiction in certain densely-packed HARS and which defined the minimal top-plate thickness required to prevent pattern collapse. Here we have expanded on

the finite elements analysis of stresses in the top-plate structures and shown that the observed breaking and plastic deformation in the structures is well modeled in our approach. Furthermore we have investigated the effect of transient forces and shown that, provided the design tolerances for the static case are met, then the structures will survive the likely maximal impulses that should be present during the drying procedure.

Acknowledgements AGP acknowledges receipt of an Australian Research Council QEII fellowship and useful discussions with A. Perri. This work was supported by the Australian Synchrotron Research Program, which is funded by the Commonwealth of Australia under the Major National Research Facilities Program.

References

Alley RL, Cuan GJ, Howe RT, Konvopoulos K (1992) The effect of release-etch processing on surface microstructure stiction. In: Solid-state sensors and actuator workshop, Hilton Head, SC, pp 202–207

Becnel C, Desta Y, Kelly K (2005) Ultra-deep X-ray lithography of densely packed SU-8 features: II. Process performance as a function of dose, feature height and post exposure bake temperature. J Micromech Microeng 15:1249–1259

Bogdanov AL, Peredkov SS (2000) Use of SU-8 photoresist for very high aspect ratio X-ray lithography. Microelectron Eng 53:493–496

Chammika NB, Bettiol AA, van Kan JA, Watt F (2003) Proton beam micromachining dose normalization for SU-8 using ionoluminescence detection. Nucl Instrum Methods Phys Res B 210:256–259

Cheong WC, Lee WM, Yuan XC, Zhang LS, Dholakia K, Wang H (2004) Direct electron-beam writing of continuous spiral phase plates in negative resist with high power efficiency for optical manipulation. Appl Phys Lett 85(23):5784–5786

Despont M, Lorenz H, Fahrni N, Brugger J, Renaud P, Vettiger P (1997) High aspect ratio ultrathick, negative-tone near-UV photoresist for MEMS applications. In: MEMS'97, IEEE, Nagoya, pp 518–522

Ehrfeld W, Lehr H (1995) Deep X-ray lithography for the production of three-dimensional microstructures from metals, polymers and ceramics. Radiat Phys Chem 45:349–365

Fischer K, Chadburi B, Guckel H, Tang CM (2000) Fabrication of two-dimensional X-ray anti-scatter grids for mammography. Proc SPIE 4145:227–234

Friedrich CR et al (1997) In: P. Rai Choudhury (ed) Handbook of microlithography, micromachining and microfabrication vol 2: micromachining and microfabrication, 1st edn. SPIE Optical Engineering Press, Bellingham, 26:315

Fujimura T, Ikeda A, Etoh S, Hattori R, Kuroki Y, Chang SS (2003) Fabrication of open-top microchannel plate using deep X-ray exposure mask made with silicon on insulator substrate. Jpn J Appl Phys 42:4102–4106

Guckel H (1996) Deep X-ray lithography for micromechanics and precision engineering. Rev Sci Instrum 67(9):3357

Jian L, Desta Y, Goettert J, Bednarzik M, Loechel B, Jin Y, Aigeldinger G, Singh V, Ahrens G, Gruetzner G, Ruhmann R, Degen R (2003) SU-8 Based Deep X-ray Lithography/LIGA. Proc SPIE 4979:394–401

Kupka RK, Bouamrane F, Cremers C, Megtert S (2000) Microfabrication: LIGA-X and applications. Appl Surf Sci 164:97–110

Kupka R, Bouamrane F, Megtert S (2003) Microfabrication of massive parallel micromirror-lenses by X-ray LIGA technique: recent advances and prospects. Microsyst Technol 10:22–28

LaBianca N, Gelorme J (1997) High aspect ratio resist for thick film applications. Proc SPIE 2438:846–852

Maboudian R, Howe RT (1997) Critical review: adhesion in surface micromechanical structures. J Vac Sci Technol A 15:1–20

Makarova OV, Tang CM, Mancini DC, Moldovan N, Divan R, Ryding DG, Lee RH (2003) Development of freestanding copper antiscatter grid using deep X-ray lithography. Microsyst Technol 9:395–398

Makarova OV, Yang G, Tang CM, Mancini DC, Divan R, Yaeger J (2004) Fabrication of collimators for gamma-ray imaging. Proc SPIE 5539:126–132

Mastrangelo CH (1997) Adhesion related failure mechanisms in micromechanical devices (invited paper). Trib Lett 3:223–238

Matthew H, Tobias K, Gyuman K, Kazuki T, Yakichi H, David M, Juergen B (2003) Micromechanical testing of SU-8 cantilevers. In: ATEM'03, JSME-MMD, Sept 10–12:1–6

Nathanson HC, Guldberg J (1975) Topologically structured thin films in semiconductor device operation. Phys Thin films 8:251–298

Niels T, Tonny S, Henri J, Rob L, Miko E (1996) Stiction in surface micromachining. J Micromech Microeng 6:385–397

Peele AG, Irving THK, Nugent KA, Mancini DC, Moldovan N, Christenson TR (2002) Production issues for high aspect ratio Lobster-eye optics using LIGA. Microsyst Technol 9:55–60

Peele AG, Shew BY, Vora KD, Li HC (2004) Overcoming SU-8 stiction in high aspect ratio structures. Microsyst Technol 11(2–3):221–224

Raccurt O, Tardif F, Arnaud d' Avitaya F, Vareine T (2004) Influence of liquid surface tension on stiction of SOI MEMS. J Micromech Microeng 14:1083–1090

Ru Feng, Farris RJ (2003) Influence of processing conditions on the thermal and mechanical properties of SU8 negative photoresist coatings. J Micromech Microeng 13:80–88

Shaw JM, Gelorme J, LaBianca N, Conley WE, Holmes SJ (1997) Negative photoresists for optical lithography. IBM J Res Dev 41:81–94

Singleton L, Bogdanov AL, Peredkov SS, Wilhelmi O, Schneider A, Cremers C, Megtert S, Schmidt A (2001) Deep x-ray lithography with the SU-8 resist. Proc SPIE 4343:182–192

Vora KD, Shew BY, Harvey EC, Hayes JP, Peele AG (2005) Specification of mechanical support structures to prevent SU-8 stiction in high aspect ratio structures. J Micromech Microeng 15:978–983